The *Red clover necrotic mosaic virus* Capsid as a Multifunctional Cell Targeting Plant Viral Nanoparticle

Dustin M. Lockney,[†] Richard N. Guenther,[†] Lina Loo,[†] Wesley Overton,[†] Ray Antonelli,[†] Jennifer Clark,[§] Mei Hu,[§] Chris Luft,[§] Steven A. Lommel,[‡,§] and Stefan Franzen*[,†,§]

Department of Chemistry and Department of Plant Pathology, North Carolina State University, Raleigh, North Carolina 27695, United States, and NanoVector, Inc., P. O. Box 98385, Raleigh, North Carolina 27624-8385, United States.
Received August 10, 2010; Revised Manuscript Received October 24, 2010

Multifunctional nanoparticles hold promise as the next generation of therapeutic delivery and imaging agents. Nanoparticles comprising many types of materials are being tested for this purpose, including plant viral capsids. It has been found that *Red clover necrotic mosaic virus* (RCNMV) can be loaded with significant amounts of therapeutic molecules with molecular weights of 600 or even greater. Formulation of RCNMV into a plant viral nanoparticle (PVN) involves the loading of cargo and attachment of peptides. In this study, we show that targeting peptides (less than 16 amino acids) can be conjugated to the capsid using the heterobifunctional chemical linker sulfosuccinimidyl-4-(*N*-maleimidomethyl)cyclohexane-1-carboxylate (Sulfo-SMCC). The uptake of both native RCNMV capsids and peptide-conjugated RCNMV was tested in the HeLa cell line for peptides with and without fluorescent labels. Uptake of RCNMV conjugate with a CD46 targeting peptide was monitored by flow cytometry. When formulated PVNs loaded with doxorubicin and armed with a targeting peptide were delivered to HeLa cells, a cytotoxic effect was observed. The ability to modify RCNMV for specific cell targeting and cargo delivery offers a method for the intracellular delivery of reagents for research assays as well as diagnostic and therapeutic applications.

INTRODUCTION

The development of nanoparticles as drug carriers has been studied extensively (*1, 2*). These nanoparticles include liposomes, dendrimers, and polymeric and inorganic nanoparticles, and have each demonstrated unique properties that are advantageous for drug delivery. The amphiphilic character of liposomes enables them to package both hydrophilic and hydrophobic drug molecules (*3*). The polymer branches of dendrimers create a large surface area for the attachment of different functional components (*4*). Biodegradable polymeric nanoparticles such as chitosan (*5*) not only managed to overcome the toxicity problem attributed to synthetic polymers, but also have been demonstrated to be efficient carriers for DNA-based vaccines (*6, 7*). Silica nanoparticles carrying plasmid DNA have been demonstrated to have the advantage of inorganic nanoparticles: stability under a range of pH and temperature conditions, providing good protection for the encapsulated cargo (*8*). While each of these nanoparticle vectors has shown promise, there is still a need for vectors that can carry a therapeutic cargo, target cells, and carry a convenient label for biodistribution studies and in vivo imaging. Plant viruses have recently shown promise for vascular imaging (*9*), drug loading (*10*−*12*), and targeting (*13*−*15*). In this report, we explore the advantages of the *Red clover necrotic mosaic virus* (RCNMV) for drug loading and cell targeting applications (*16*).

Virus particles are self-assembled nanoparticles with unique features that can be exploited for medical applications (*17*). The symmetrical outer surface of a virus is a versatile platform that can be used to display various signals such as peptides, protein, fluorescent labels, or chelating groups (*18*−*22*). These display signals can be developed as cell-targeting or bioimaging agents by appropriate modification with organic dyes or inorganic complexes (*23*−*25*). For example, the fluorescently labeled *Cowpea mosaic virus* (CPMV) has been used for intravital vascular imaging in mouse and chick embryos (*9*), as well as a template for synthesis of magnetic particles (*26*). The conjugation of CD46 (cellular receptor of measles virus) to CPMV was shown to function as an antiviral agent to inhibit the measles virus infection efficiently in vitro (*27*). Moreover, the rigidity and robustness of the virus capsids can be exploited as a container for encapsulation of other nanoparticles (*28, 29*), as well as drug molecules (*10, 30*). Other protein cages such as the human ferritin cage have also been demonstrated to package magnetic nanoparticles along with an externally conjugated RGD peptide, for cell-specific targeting (*24*). The ability to impart functionality to the outer surface, together with the loading capacity, have combined to make protein cages a tool for development as drug delivery vectors.

RCNMV belongs to the *Dianthovirus* genus and *Tombusviridae* family. RCNMV is a $T = 3$ icosahedral soil-transmitted virus with a diameter of 36 nm. The capsid of RCNMV consists of 180 copies of capsid protein that assembles to package either 1 copy each of a 3.9 kb single-stranded RNA-1 and a 1.5 kb RNA-2 or 4 copies of RNA-2 (*31*). The RCNMV capsid has been demonstrated as a versatile container to package various composites of nanoparticles in the diameter range 3−15 nm using RNA-dependent packaging (*32*) based on the origin of assembly of RCNMV (*33, 34*). The opening of surface pores under control of the Ca^{2+} and Mg^{2+} concentrations has been demonstrated as a method to package molecules inside the RCNMV capsid. Cryo-electron microscopy provides a molecular-level description of the mechanism whereby the RCNMV capsid undergoes a structural transition in response to divalent-

* To whom correspondence should be addressed. Stefan Franzen, Department of Chemistry, North Carolina State University, Raleigh, NC 27695.
[†] Department of Chemistry, North Carolina State University.
[‡] Department of Plant Pathology, North Carolina State University.
[§] NanoVector, Inc.

10.1021/bc100361z
Published on Web 12/02/2010

Table 1. Sequences and Fluorophores for Peptides Used in Cell Uptake Studies

peptide abbreviation	sequence	fluorophore	peptides/PVN
$CD46^{rev}$-F	CGGFSTSLRARKA	fluorescein	115 ± 8
RME-F	CKKKKKKSEDEY	fluorescein	146 ± 19
IBD-R	CKKKKKKGGRGD	rhodamine	224 ± 40
CD46-F	AKRARLSTSFGGC	fluorescein	100 ± 20

cation concentration, leading to the formation of surface pores extending through the capsid (*35*). The transition in virus structure in response to cytoplasmic levels of these divalent cations is associated with the release mechanism of the bipartite RNA genome in vivo.

Cell targeting for gene therapy and for drug delivery depends upon recognition of cell surface receptors. In this study, we have used adenoviral sequences for an initial screen of internalization in cells. The adenoviral fiber targets cell surface receptors in a serotype-dependent manner (*36, 37*). In nature, the fiber protein of adenovirus serotypes subgroup C and subgroup B bind to CAR (*38*) and CD46 (*39*) receptors, respectively, followed by interaction of the RGD (Arg-Gly-Asp) sequence from the penton base with the integrins on the cell surface for internalization (*40*). In an attempt to mimic the internalization of an adenovirus, synthetic peptides consisting of the RGD sequence or peptides that bind to CAR or CD46 receptors have been conjugated to liposomes (*41*) or nanoparticles (*42*). Targeting of cancer cells depends on the determination of a specific cell surface receptor that is overexpressed. The fact that adenovirus targets healthy cells, and that certain receptors such as CAR are actually repressed in the cancer cell phenotype, has led to a search for targeting motifs that are more specific (*43, 44*). In this study, we used an N-cadherin targeting sequence in cell targeting studies as a demonstration of the potential of such specific uptake for increased delivery of a doxorubicin payload to a cancer cell (*45*). The switch from E-cadherin to N-cadherin expression is a phenotype transition common to many cancers, especially in advanced cancers, that presents a possible target for selective delivery to these cancer cells (*46*).

The use of RCNMV to prepare a PVN formulation to target cancer cells involves two steps. First, the capsid must be infused with a chemotherapeutic cargo. We previously demonstrated that RCNMV has a specific and high loading density when doxorubicin is used as the cargo (*11*). In the present study, we show that PVN loaded with doxorubicin can also be functionalized to targeting peptide using heterobifunctional linkers. Furthermore, the cytotoxic effect when such formulations are incubated with HeLa cells can be used as a measure of the specificity of cell targeting. In these studies, we find that N-cadherin targeting peptides provide a significantly greater cytotoxic effect than the RME, IDB, and CD46 (Table 1) peptides previously used in targeting studies of HeLa cells (*47, 48*). To test this, a linear peptide was employed that contains the HAV sequence, an essential sequence for N-cadherin targeting (*45*). The combination of infused cargo and surface-attached targeting peptides is a step toward a multifunctional plant virus nanoparticle capable of targeting cancer cells.

EXPERIMENTAL PROCEDURES

Nomenclature. The term PVN will be used to denote formulated RCNMV particles. The following nomenclature will be used to denote the different PVN formulations. A cargo internalized in the PVN will precede the PVN as a superscript, e.g., ^{Dox}PVN for doxorubicin-loaded PVN. Any surface formulation will be denoted as a superscript following the PVN term, e.g., PVN^{CD46} for a PVN labeled with CD46 targeting peptide. A PVN that contains doxorubicin in the interior and has a CD46 targeting peptide on the surface will be denoted as $^{Dox}PVN^{CD46}$.

RCNMV Propagation and Purification. Growth in host plants and subsequent purification of RCNMV were carried out as described previously (*35*). In brief, RCNMV RNA transcripts were inoculated on *Nicotiana clevelandii* plants and maintained under standard greenhouse conditions for 7 to 10 days. Virions were collected from infected leaves and purified. The concentration of virus was determined by absorbance measurement at 260 nm with an extinction coefficient of 6.46 mL mg^{-1} cm^{-1}.

Preparation of RCNMV-Infused Doxorubicin (^{Dox}PVN). Native RCNMV, stored in 200 mM NaOAC pH 5.5, was diluted to 5 mg/mL in water. 2 M Tris-HCl and 1 M EDTA were added to bring final buffer concentration to 50 mM NaOAC, 50 mM TRIS-HCl, and 50 mM EDTA at pH 8.0. The virus suspension was incubated in buffer for 30 min at room temperature. Doxorubicin (500 μM) was infused into RCNMV (5 mg/mL) overnight at room temperature. After overnight incubation, 1 M sodium acetate, 25 mM $CaCl_2$, and 25 mM $MgCl_2$ were added to the virus suspension and incubated for an additional 30 min at RT. Excess molecules were removed by NAP 25 columns, pre-equilibrated with 50 mM HEPES, pH 7.2. Absorbance at 260 nm was measured from 0.5 mL fractions. The fractions with the highest absorbance value were collected and pooled. Loading of doxorubicin in RCNMV as high as 1000 molecules per virion has been reported (*11*). Routine and highly reproducible loadings of ~900 were achieved in these studies. Samples were syringe filter sterilized (0.2 μm Whatman) prior to use in cell culture media.

Conjugation of Fluorescently Labeled Peptide to RCNMV ($PVN^{peptides}$). Fluorescently labeled peptides were custom-made at the UNC Microprotein Sequencing & Peptide Synthesis Facility (Chapel Hill, NC). Each peptide contained a cysteine at the N-terminal and was fluorescently labeled with fluorescein or rhodamine at the N-terminus. One milligram per milliliter of RCNMV was incubated with sulfosuccinimidyl-4-(*N*-maleimidomethyl) cyclohexane-1-carboxylate (Sulfo-SMCC) (Pierce) at a mole ratio of 1:300 (RCNMV-to-Sulfo-SMCC). The solution volume was brought up to 1 mL with 1× Dulbecco's phosphate buffered saline with calcium and magnesium (DPBS) and incubated for 30 min at room temperature. Excess Sulfo-SMCC was removed by centrifugation at 13 200 rpm for 10 min with a Microcon-30K (Millipore, Billerica, MA). RCNMV-SMCC conjugates were then incubated with fluorescently labeled peptide at a mole ratio of 1:300 (RCNMV-SMCC conjugates-to-peptide) and DPBS added to achieve a final volume of 1 mL, followed by incubation for 6 h at room temperature. Excess peptides were removed using a Microcon-30K filter (Millipore, Billerica, MA) via centrifugation at 13 200 rpm for 10 min, and this step was repeated until the filtrate was devoid of fluorescence. Standard curves of fluorescently labeled peptides were generated to quantify the number of peptides per PVN. Conjugation of peptide ligands to proteins is typically achieved by chemical ligation to solvent-accessible lysine or cysteine residues. The sequence of the RCNMV capsid protein (CP) has 16 lysine and 5 cysteine residues as potential targets for peptide conjugation (*35*). Inspection of the cryo-EM reconstruction model of the RCNMV CP subunit reveals that each subunit contains two lysine residues and one cysteine residue (colored red and blue, respectively; see Figure 1A) that are located within the protruding domains on the capsid exterior and appear most accessible for peptide conjugation (*35*). In this study, we conjugated fluorescently labeled peptides to the PVN using Sulfo-SMCC to monitor uptake into HeLa cells using flow cytometry, and we used nonfluorescently labeled peptides in order to determine the cytotoxic effect of doxorubicin-infused PVN in vitro. The fluorescently labeled peptides were designated RME-F, IBD-R, CD46-F, and the reverse of CD46-F, which is $CD46^{rev}$-F (See Table 1). The $CD46^{rev}$ sequence is the reverse

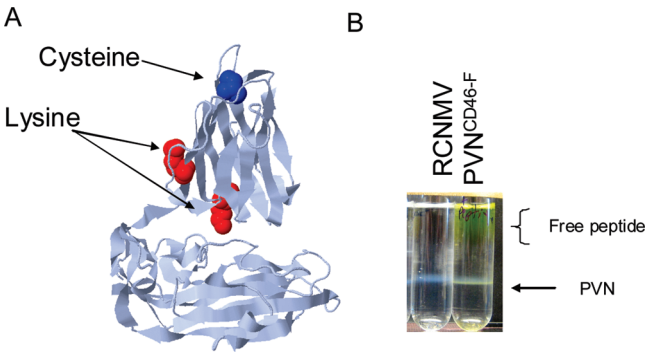

Figure 1. Conjugation of fluorescently labeled peptides onto the RCNMV capsid. (A) Subunit ribbon diagram. Two lysine residues, indicated in red, and one cysteine appear to be exposed on the outer surface of the capsid. (B) The Optiprep gradient centrifugation of a conjugation reaction suggests peptide conjugation to the PVN.

Table 2. Effect of Number of Peptides Per Capsid and Average Fluorescence

peptides per PVN	control	8	12	20	40	60
mean cell fluorescence[a]	14.5	25	36.6	39.6	46.7	55.6

[a] Mean for 10 000 events.

of the CD46 sequence and was discovered to have similar uptake (see Supporting Information).

Conjugation of Nonfluorescently Labeled Peptides to Doxorubicin-Loaded PVN ($^{DOX}PVN^{peptides}$). Nonfluorescently labeled peptides were obtained from Genscript, Inc. The CD46_1 peptide (AKRARLSTSFC) differed from the fluorescently labeled peptide in that it also lacks two glycines, serving as a spacer in the peptide sequence shown in Tables 1 and 2. Bioconjugation protocols using Sulfo-SMCC were conducted as above for the fluorescently labeled peptides. The coupling of nonfluorescently labeled peptides was established by polyacrylamide gel electrophoresis of the 37 kDa capsid protein (Supporting Information Figure S7). In addition to the CD46 sequence, as is reported in Table 1, the ADH304 sequence, Ac-FHLRAHAVDINGNQVC-NH_2, was used to target HeLa cells. The target for the ADH304 sequence is N-cadherin, which is present on many cancer cells that have undergone the epithelial−mesenchymal transition, also known as the E-cadherin to N-cadherin switch, a change that leads to loss of cell adhesion and greater migration potential (*47, 48*). This transition is an essential step in metastasis, and ADH304 was chosen to bind to a specific test target for the delivery of doxorubicin. The gel in Supporting Information Figure S7 shows that the heterobifunctional coupling yield of the CD46 and ADH304 peptides is greater than one per capsid, which implies >180 per PVN.

Cell Culture. HeLa (human cervical cancer) cells were purchased from American Type Culture Collection (Rockville, MD). Minimum Essential Medium Eagle (EMEM), fetal bovine serum (FBS), DPBS, T-25, and T-75 cell culture flasks were purchased from Bio-Whittaker, Inc. (Walkersville, MD). HeLa and HepG2 cells were cultured in Minimum Essential Medium Eagle (EMEM) media containing 10% fetal bovine serum and 1% penicillin−streptomycin at 37 °C in an atmosphere containing 5% CO_2. To plate the cells into a well plate, the culture media was removed, and cells were washed with DPBS twice before harvesting using 5% trypsin (Gibco Laboratories, Gaithersburg, MD) solution. Then, cells were seeded ∼10 000 cells/well in a 6-well plate and incubated at 37 °C for 24 h before experiments were performed.

Flow Cytometry. Cells were analyzed by a fluorescence-activated cell sorter (Becton Dickinson, FACScalibur) equipped with an argon laser (488 nm) using *Cell Quest* software. Cells suspended in media were introduced into the flow stream at a flow rate of ∼120 μL/minute. Results were based on the signal acquisition corresponding to 10 000 cells. The relative fluorescence intensity was calculated by dividing the mean fluorescence intensity of treated sample with the mean fluorescence intensity of untreated sample. Data are represented as the mean of triplicates with the error bars representing the standard deviation.

RESULTS

Formulation of PVN Using Fluorescently Labeled Peptides. Conjugation of targeting peptides to the capsid, listed in Table 1, was confirmed using fluorescence, gel electrophoresis, and Optiprep step gradient centrifugation. Centrifugation through a 0−60% Optiprep step gradient shows a visibly colored band (Figure 1B) at the approximate density of RCNMV. The colored band is just below the native control sample, indicating a slight increase in density, possibly due to the increase in mass from the conjugated peptides. An additional confirmation of peptide conjugation to the PVN was found when formulated material was introduced to a 25 kDa molecular weight cutoff Microcon filter. The PVN remained in the retentate and could be washed until no fluorescence was observed in the filtrate. Following collection of the retentate, the number of peptides conjugated per PVN was calculated by dividing the peptide concentration by the PVN concentration determined by fluorescence and UV−vis absorbance, respectively. Table 1 contains a summary of the conjugation efficiency for the fluorescent peptides. In general, an average of somewhat less than one peptide per CP subunit was observed. To determine if the combination of infusion of molecules and peptide conjugation disrupted the capsid integrity, additional characterizations by transmission electron microscopy (TEM) and dynamic light scattering (DLS) were performed (see Supporting Information). The images of the native RCNMV and the PVN obtained by TEM show little change in the particle morphology (Supporting Information Figure S3). Comparison of the average particle size found by DLS showed a small increase in diameter from 34.0 ± 3 nm (*32*) to 37.6 ± 4 nm, which may reflect the addition of the peptide lengths to the overall diameter of the PVN (Supporting Information Figure S3).

PVNs with Conjugated Peptides Are Internalized by HeLa Cells in a Peptide-Dependent Manner. PVN uptake in cells was quantified using flow cytometry. It was determined at an early stage that the PVN^{CAR-F} and PVN^{IBD-F} formulations were not internalized to a significant extent (see Supporting Information). Therefore, a more detailed comparison was made of the PVN^{CD46-F} and $PVN^{CD46rev-F}$ formulations with controls (Figure 2). Cells, grown in a 24 well plate to near confluency, were dosed with PVN over a concentration range of 1×10^{-7} M to 4×10^{-9} M for a 3 h exposure. Cells were removed from the plate by treatment with trypsin and analyzed within one hour. Figure 2A shows cell fluorescence histograms, and the number of cells per cell fluorescence intensity for both $PVN^{CD46rev-F}$ and PVN^{CD46-F}, at 3 h postdosing, show an upward shift in average fluorescence. This shift was not seen in nondosed or RCNMV and PVN^{FITC} dosed controls. The shift in the fluorescence signal measured by flow cytometry was dependent on both the number of peptides conjugated per PVN and the concentration of PVN. When a serial dilution of a PVN^{CD46-F} was performed and tested, the fluorescence histograms exhibited a concentration-dependent shift, indicating that PVN uptake was dose-dependent (Figure 2B). Uptake also was found to depend on the number of CD46 targeting peptides conjugated to the PVN (Table 2).

Testing the Bioavailability of Doxorubicin Infused in a Targeting PVN. To determine whether the formulated PVN could deliver a payload to a cell, PVNs were formulated with

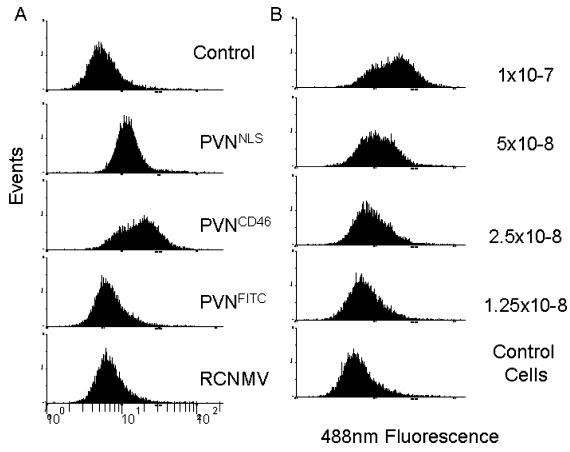

Figure 2. Flow cytometry plots. (A) Cell fluorescence histograms show increases for cells dosed with $PVN^{CD46rev\text{-}F}$ and $PVN^{CD46\text{-}F}$ but not for nonformulated RCNMV or PVN^{FITC}. (B) A histogram for cells dosed with different concentrations of $PVN^{CD46\text{-}F}$ shows a dose-dependent fluorescence shift.

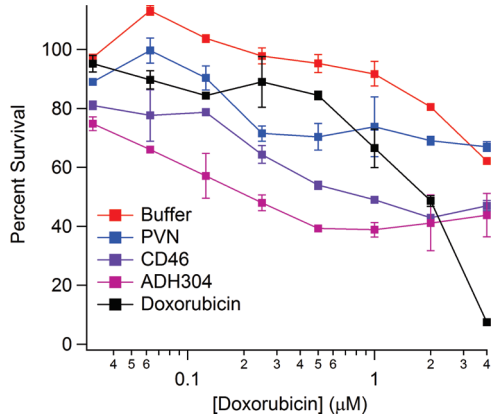

Figure 3. Cell targeting survivability of HeLa cells after 72 h of continuous exposure in the presence of various $^{Dox}PVN^{peptide}$ formulations.

a doxorubicin cargo and two targeting peptides, CD46 and ADH304, providing: $^{Dox}PVN^{CD46}$ and $^{Dox}PVN^{ADH304}$, respectively. The formulated PVN were delivered to HeLa cells grown to near-confluency in a 96 well plate. Cells were dosed using PVN concentrations that ranged from 1×10^{-12} to 1×10^{-7} M. For the purpose of clarity, the dosage will be reported based on the doxorubicin concentration to enable easy comparison to the free drug control. After 72 h of continuous exposure, the viability of the dosed cells was measured with an alamarBlue assay. Figure 3 shows the dose response of the cells to increasing concentrations of doxorubicin. In addition, two formulation intermediates: infused only (^{Dox}PVN) and PVN with SMCC only (PVN^{SMCC}) were also tested (see Supporting Information). The EC_{50} for doxorubicin was observed to be 1.02 ± 0.5. Although an increase in cytotoxicity was observed in the formulations with targeting peptides, this increase was time-dependent (Figure 3). Moreover, the behavior of the PVN formulations is not nearly as well-defined as in a typical dose−response curve. For $^{Dox}PVN^{CD46}$, free doxorubicin, and PVN^{SMCC}, detectable toxicity was observed. The toxicity of the $^{Dox}PVN^{CD46}$ was greater than that for the free doxorubicin and PVN^{SMCC}.

DISCUSSION

In this report, we describe an approach to use RCNMV capsid to target and deliver molecules into cancer cells. When modified by infusion of a drug or cargo and conjugation of targeting peptides, the resulting modified virus is termed a PVN. On the basis of cross-linking chemistry, the capsid of RCNMV was conjugated with targeting peptides, with average numbers of peptides ranging from 100 to 220 per PVN for the fluorescently labeled peptides used to test for internalization in HeLa cells. Although the quantification is less precise using gel electrophoresis, we have observed higher levels of loading using nonfluorescently labeled peptides infused with doxorubicin. These results indicate that a targeting peptide is required in order to facilitate internalization or cytotoxic effect. This is advantageous as the targeting peptide confers specificity of intracellular uptake to the PVN. This type of uptake can be contrasted with the internalization of CPMV, which has the natural ability to bind to 54 kDa and 47 kDa membrane proteins on mammalian cells resulting in localization in vascular endothelial cells (*49*). RCNMV has no known uptake mechanism in cells unless a targeting peptide is chemically attached to its surface. The present work suggests the advantage of introducing targeting capability onto the surface of a plant virus nanoparticle that lacks intrinsic targeting ability.

Nanoparticles are ideal drug carriers because the diameters on the nanometer scale promote tumor permeability and retention (*50*). The size of a drug carrier not only affects the intracellular uptake, but also the efficiency for drug encapsulation or attachment (*51*). Although the synthesis of inorganic nanoparticles can be carried out in high yield, it remains a challenge to obtain a narrow size distribution (*52*). A number of variables such as solvent composition, pH, and temperature determine the size and polydispersity of nanoparticles in such preparations. As opposed to inorganic nanoparticles, the homogeneity in size and shape as well as the ease of production of RCNMV are advantageous for biomedical applications.

The structural model of RCNMV based on the cryo-EM structure suggests that two surface-exposed lysines per CP, a total of 360 per PVN, should be accessible for conjugation. The observed peptide conjugation numbers were significantly less than this value, likely due the limited reactivity of the two most solvent-accessible lysines on the surface of RCNMV (K209 and K218). The positions of these lysines were determined by homology modeling of the X-ray crystal structures for *Carnation mottle virus* (*53*) and *Tomato bushy stunt virus* (*54*) into the electron density determined in the cryo-EM structure of RCNMV (*35*). These two lysines are near the base of the P-domain, which is not the optimal location for peptide binding, but nonetheless surface exposed and somewhat elevated relative to the capsid shell. The reactivity of solvent-accessible lysine on a plant viral capsid can vary significantly. An extensive characterization of the reactivity of the surface lysines of CPMV found that the reactivity of any individual residue can range from less than 10% to greater than 90% (*55*), which led to the genetic modification to create reactive lysine positions on the capsid (*56*). Engineering or sometimes fortuitous positions, e.g., at the N-terminus, can promote highly efficient heterobifunctional cross-linking by SMCC (*57*). The approach used here can be extended to a large number of different targeting peptides and ligands for specific cell types with a coupling efficiency of approximately 28−33% (i.e., 110−120 peptides conjugate per 360 lysines). Other targeting signals including folic acid (*13*), HER-2, and Large T (*47*) are likely to be effective in facilitating RCVNV uptake.

Despite its ease of use and reasonable yield, Sulfo-SMCC has several disadvantages that were encountered in the present study. First, there was some evidence for cross-linking of capsid proteins in RCNMV based on gel electrophoresis (Supporting Information Figure S7). Although a relatively small fraction of the total coat proteins is affected, cross-linking is nonetheless undesirable since it reduces peptide conjugation yield and may prevent cargo release in cells. A second disadvantage is the

uptake of Sulfo-SMCC-labeled PVNs, PVN^{SMCC}. Although the maleimide should hydrolyze to a significant extent during the process of the cell delivery, any unreacted site on a Sulfo-SMCC conjugated PVN can potentially give rise to nonspecific cell adhesion and uptake. This experience suggests that "click" chemistry or genetic modification may provide more viable methods for future experiments (*58*−*61*).

The capability to modify the RCNMV capsid both internally and externally while maintaining capsid integrity indicates the robustness of RCNMV as a nanoparticle vessel for the transport of therapeutic cargo. It is critical to protect the cargo during endocytosis in order to maintain the drug's therapeutic activity during the delivery process. In comparison, one major concern of liposomes as drug carriers is the instability of liposomal formulation due to oxidation and hydrolysis of lipids, as well as aggregation or fusion of particles (*62*). The use of poly(ethylene glycol) (PEG) on liposomes has been reported to minimize plasma clearance and further increase the circulation time (*63*). However, drug leakage was reported for liposomal doxorubicin formulation (*64*), which may influence the therapeutic index of the drug formulation. It is desirable to overcome these obstacles with pH-dependent triggered release, as has been demonstrated using modified lipids (*65*). RCNMV is a soil-borne virus with a capsid that has evolved to package and protect the viral genome against the harsh environment found in soils at low pH. This virus is equipped with a natural pH and ion sensor that enables it to release its RNA genome in the pH and ionic conditions of cytosol. These features have been used to control the synthesis of PVNs and also to facilitate the transport of molecules into the cytosol as demonstrated in Figures 2 and 3.

The sensitivity of RCNMV to divalent cation concentration is a unique advantage for drug delivery applications. Divalent ions act as a switch to open and close surface pores (*35*). In blood, where the Ca^{2+} and Mg^{2+} concentrations are in the millimolar range, the capsid stays intact with the cargo package. In the endosome where the pH is low (<6.0), RCNMV is also stable. Only in the cytosol, where the Ca^{2+} and Mg^{2+} concentrations are sufficiently low, do the surface pores open with concomitant release of the cargo. In comparison, drug released from most polymeric micelles or liposomes often involves the assistance of physical fields such as low-frequency ultrasound (*66*) or irradiation with light (*67*). Clever synthetic strategies can also provide pH-triggered release in the endosome (*65*). In contrast to these release mechanisms, RCNMV has a natural release mechanism that is required for RNA release from the capsid as part of the viral life cycle. The low toxicity of ^{Dox}PVN control suggests that leakage in growth media is not significant for the nontargeting doxorubicin formulation.

Aggregation and precipitation are recurring problems in complex PVN formulations that involve an infused drug, Sulfo-SMCC, and conjugated peptides. Avoiding precipitation is a key aspect of process optimization for the preparation of PVNs in high yield. Aside from consideration of the need to keep ionic strength low, one must be mindful that the isoelectric point of RCNMV is ∼6.4. Since this is relatively close to neutral pH, aggregation and precipitation are often observed in this pH range. Despite these issues, PVNs are almost entirely organic (aside from bound Ca^{2+} and Mg^{2+}) and consequently have relatively small van der Waals interactions. PVNs have significantly greater colloidal stability than gold, metal oxide, or II−VI semiconductor nanoparticles. We have observed that presentation of targeting peptides in PVNs permits targeting similar to that observed in gold nanoparticles (*47, 48, 68*), with the added advantage of an ability to load a chemical cargo in the PVN interior (*11*). This approach is superior to attachment of cargo to the surface of solid nanoparticles, which has been shown to result in loss of function of the cargo in some cases (*69*).

In summary, we have demonstrated that the RCNMV capsid can be employed as a multifunctional tool to target and deliver chemotherapy agents. The modification of the RCNMV capsid to provide a nanoparticle loaded with cargo and armed with targeting peptides has been demonstrated in the ability to deliver cargo to cancer cells. The combination of drug sequestration in the interior and targeting peptides on the exterior has only recently been realized in nanoparticle formulations. While synthesis of modified copolymers or lipids containing a targeting agent has permitted targeting in those systems, plant virus nanoparticles offer the advantage of small diameter (36 nm), uniformity of size and shape, and the potential for natural triggered release due to cytosolic conditions. It is not yet clear whether these advantages will compete with the well-established methods, but this study demonstrates the viability of plant viruses for cell targeting.

ACKNOWLEDGMENT

We thank Janet Dow in the College of Veterinary Medicine for help with flow cytometry and Dr. Tim Sit for help with the RCNMV molecular biology. We thank Dr. Ambrose Wallace in the School of Dentistry at UNC for help with TEM. We thank Dr. Bruce Oberhardt of Nanovector, Inc., for a critical reading of the manuscript and insightful comments.

Supporting Information Available: Plate reader, flow cytometry, and light microscopy data are available to document uptake of $^{Dox}PVN^{CD46rev}$ formulations. TEM and DLS data for characterization of the formulations are available. This material is available free of charge via the Internet at http://pubs.acs.org.

LITERATURE CITED

(1) Torchilin, V. P. (2006) Multifunctional nanocarriers. *Adv. Drug Delivery Rev. 58*, 1532–1555.
(2) Kayser, O., Lemke, A., and Hernandez-Trejo, N. (2005) The impact of nanobiotechnology on the development of new drug delivery systems. *Curr. Pharm. Biotechnol. 6*, 3–5.
(3) Rawat, M., Singh, D., Saraf, S., and Saraf, S. (2006) Nanocarriers: Promising vehicle for bioactive drugs. *Biol. Pharm. Bull. 29*, 1790–1798.
(4) Frechet, J. M. J. (1994) Functional polymers and dendrimers - reactivity, molecular architecture, and interfacial energy. *Science 263*, 1710–1715.
(5) Fernandez-Urrusuno, R., Calvo, P., Remunan-Lopez, C., Vila-Jato, J. L., and Alonso, M. J. (1999) Enhancement of nasal absorption of insulin using chitosan nanoparticles. *Pharm. Res. 16*, 1576–1581.
(6) Kim, T. H., Park, I. K., Nah, J. W., Choi, Y. J., and Cho, C. S. (2004) Galactosylated chitosan/DNA nanoparticles prepared using water-soluble chitosan as a gene carrier. *Biomaterials 25*, 3783–3792.
(7) Aktas, Y., Andrieux, K., Alonso, M. J., Calvo, P., Gursoy, R. N., Couvreur, P., and Capan, Y. (2005) Preparation and in vitro evaluation of chitosan nanoparticles containing a caspase inhibitor. *Intl. J. Pharm. 298*, 378–383.
(8) Luo, D., Han, E., Belcheva, N., and Saltzman, W. M. (2004) A self-assembled, modular DNA delivery system mediated by silica nanoparticles. *J. Controlled Release 95*, 333–341.
(9) Lewis, J. D., Destito, G., Zijlstra, A., Gonzalez, M. J., Quigley, J. P., Manchester, M., and Stuhlmann, H. (2006) Viral nanoparticles as tools for intravital vascular imaging. *Nat. Med. 12*, 354–360.
(10) Ren, Y., Wong, S. M., and Lim, L. Y. (2007) Folic acid-conjugated protein cages of a plant virus: A novel delivery platform for doxorubicin. *Bioconjugate Chem. 18*, 836–843.
(11) Loo, L., Guenther, R. H., Lommel, S. A., and Franzen, S. (2008) Infusion of dye molecules into Red clover necrotic mosaic virus. *Chem. Commun.* 88–90.

(12) Flenniken, M. L., Liepold, L. O., Crowley, B. E., Willits, D. A., Young, M. J., and Douglas, T. (2005) Selective attachment and release of a chemotherapeutic agent from the interior of a protein cage architecture. *Chem. Commun.* 447–449.
(13) Destito, G., Yeh, R., Rae, C. S., Finn, M. G., and Manchester, M. (2007) Folic acid-mediated targeting of cowpea mosaic virus particles to tumor cells. *Chem. Biol. 14*, 1152–1162.
(14) Gillitzer, E., Suci, P., Young, M., and Douglas, T. (2006) Controlled ligand display on a symmetrical protein-cage architecture through mixed assembly. *Small 2*, 962–966.
(15) Gillitzer, E., Willits, D., Young, M., and Douglas, T. (2002) Chemical modification of a viral cage for multivalent presentation. *Chem. Commun.* 2390–2391.
(16) Franzen, S., and Lommel, S. A. (2009) Targeting cancer with 'smart bombs': equipping plant virus nanoparticles for a 'seek and destroy' mission. *Nanomedicine 4*, 575–588.
(17) Singh, P., Prasuhn, D., Yeh, R. M., Destito, G., Rae, C. S., Osborn, K., Finn, M. G., and Manchester, M. (2007) Bio-distribution, toxicity and pathology of cowpea mosaic virus nanoparticles in vivo. *J. Controlled Release 120*, 41–50.
(18) Soto, C. M., Blum, A. S., Vora, G. J., Lebedev, N., Meador, C. E., Won, A. P., Chatterji, A., Johnson, J. E., and Ratna, B. R. (2006) Fluorescent signal amplification of carbocyanine dyes using engineered viral nanoparticles. *J. Am. Chem. Soc. 128*, 5184–5189.
(19) Chatterji, A., Ochoa, W. F., Ueno, T., Lin, T. W., and Johnson, J. E. (2005) A virus-based nanoblock with tunable electrostatic properties. *Nano Lett. 5*, 597–602.
(20) Allen, M., Bulte, J. W. M., Liepold, L., Basu, G., Zywicke, H. A., Frank, J. A., Young, M., and Douglas, T. (2005) Paramagnetic viral nanoparticles as potential high-relaxivity magnetic resonance contrast agents. *Magn. Res. Med. 54*, 807–812.
(21) Wang, Q., Kaltgrad, E., Lin, T. W., Johnson, J. E., and Finn, M. G. (2002) Natural supramolecular building blocks: Wild-type cowpea mosaic virus. *Chem. Biol. 9*, 805–811.
(22) Steinmetz, N. F., Mertens, M. E., Taurog, R. E., Johnson, J. E., Commandeur, U., Fischer, R., and Manchester, M. (2009) Potato virus X as a novel platform for potential biomedical applications. *Nano Lett. 10*, 305–312.
(23) Evans, D. J. (2010) Bionanoscience at the plant virus-inorganic chemistry interface. *Inorg. Chim. Acta 363*, 1070–1076.
(24) Uchida, M., Flenniken, M. L., Allen, M., Willits, D. A., Crowley, B. E., Brumfield, S., Willis, A. F., Jackiw, L., Jutila, M., Young, M. J., and Douglas, T. (2006) Targeting of cancer cells with ferrimagnetic ferritin cage nanoparticles. *J. Am. Chem. Soc. 128*, 16626–16633.
(25) Basu, G., Allen, M., Willits, D., Young, M., and Douglas, T. (2003) Metal binding to cowpea chlorotic mottle virus using terbium(III) fluorescence. *J. Biol. Inorg. Chem. 8*, 721–725.
(26) Aljabali, A. A. A., Sainsbury, F., Lomonossoff, G. P., and Evans, D. J. (2010) Cowpea mosaic virus unmodified empty viruslike particles loaded with metal and metal oxide. *Small 6*, 818–821.
(27) Khor, I. W., Lin, T. W., Langedijk, J. P. M., Johnson, J. E., and Manchester, M. (2002) Novel strategy for inhibiting viral entry by use of a cellular receptor-plant virus chimera. *J. Virol. 76*, 4412–4419.
(28) Chen, C., Kwak, E. S., Stein, B., Kao, C. C., and Dragnea, B. (2005) Packaging of gold particles in viral capsids. *J. Nanosci. Nanotechnol. 5*, 2029–2033.
(29) Douglas, T., and Young, M. (1998) Host-guest encapsulation of materials by assembled virus protein cages. *Nature 393*, 152–155.
(30) Kovacs, E. W., Hooker, J. M., Romanini, D. W., Holder, P. G., Berry, K. E., and Francis, M. B. (2007) Dual-surface-modified bacteriophage MS2 as an ideal scaffold for a viral capsid-based drug delivery system. *Bioconjugate Chem. 18*, 1140–1147.
(31) Basnayake, V. R., Sit, T. L., and Lommel, S. A. (2006) The genomic RNA packaging scheme of red clover necrotic mosaic virus. *Virology 345*, 532–539.
(32) Loo, L., Guenther, R. H., Lommel, S. A., and Franzen, S. (2007) Encapsidation of nanoparticles by red clover necrotic mosaic virus. *J. Am. Chem. Soc. 129*, 11111–11117.
(33) Guenther, R. H., Sit, T. L., Gracz, H. S., Dolan, M. A., Townsend, H. L., Liu, G. H., Newman, W. H., Agris, P. F., and Lommel, S. A. (2004) Structural characterization of an intermolecular RNA-RNA interaction involved in the transcription regulation element of a bipartite plant virus. *Nucleic Acids Res. 32*, 2819–2828.
(34) Sit, T. L., Vaewhongs, A. A., and Lommel, S. A. (1998) RNA-mediated trans-activation of transcription from a viral RNA. *Science 281*, 829–832.
(35) Sherman, M. B., Guenther, R. H., Tama, F., Sit, T. L., Brooks, C. L., Mikhailov, A. M., Orlova, E. V., Baker, T. S., and Lommel, S. A. (2006) Removal of divalent cations induces structural transitions in Red clover necrotic mosaic virus, revealing a potential mechanism for RNA release. *J. Virol. 80*, 10395–10406.
(36) Lanford, R. E., Feldherr, C. M., White, R. G., Dunham, R. G., and Kanda, P. (1990) Comparison of diverse transport signals in synthetic peptide-induced nuclear transport. *Exp. Cell Res. 186*, 32–38.
(37) Jans, D. A., Chan, C. K., and Huebner, S. (1998) Signals mediating nuclear targeting and their regulation: Application in drug delivery. *Med. Res. Rev. 18*, 189–223.
(38) Bergelson, J. M., Cunningham, J. A., Droguett, G., KurtJones, E. A., Krithivas, A., Hong, J. S., Horwitz, M. S., Crowell, R. L., and Finberg, R. W. (1997) Isolation of a common receptor for coxsackie B viruses and adenoviruses 2 and 5. *Science 275*, 1320–1323.
(39) Sirena, D., Lilienfeld, B., Eisenhut, M., Kalin, S., Boucke, K., Beerli, R. R., Vogt, L., Ruedl, C., Bachmann, M. F., Greber, U. F., and Hemmi, S. (2004) The human membrane cofactor CD46 is a receptor for species B adenovirus serotype 3. *J. Virol. 78*, 4454–4462.
(40) Wickham, T. J., Mathias, P., Cheresh, D. A., and Nemerow, G. R. (1993) Integrin-alpha-v-beta-3 and integrin-alpha-v-beta-5 promote adenovirus internalization but not virus attachment. *Cell 73*, 309–319.
(41) Yagi, N., Ogawa, Y., Kodaka, M., Okada, T., Tomohiro, T., Konakahara, T., and Okuno, H. (2000) Preparation of functional liposomes with peptide ligands and their binding to cell membranes. *Lipids 35*, 673–680.
(42) Chorny, M., Fishbein, I., Alferiev, I. S., Nyanguile, E., Gaster, R., and Levy, R. J. (2006) Adenoviral gene vector tethering to nanoparticle surfaces results in receptor-independent cell entry and increased transgene expression. *Mol. Ther. 14*, 382–391.
(43) Dmitriev, I., Krasnykh, V., Miller, C. R., Wang, M. H., Kashentseva, E., Mikheeva, G., Belousova, N., and Curiel, D. T. (1998) An adenovirus vector with genetically modified fibers demonstrates expanded tropism via utilization of a coxsackievirus and adenovirus receptor-independent cell entry mechanism. *J. Virol. 72*, 9706–9713.
(44) Yamamoto, M., and Curiel, D. T. (2010) Current issues and future directions of oncolytic adenoviruses. *Mol. Ther. 18*, 243–250.
(45) Kelland, L. (2007) N-cadherin: a novel target for cancer therapy? *Drugs Future 32*, 925–930.
(46) Cavallaro, U., and Christofori, G. (2004) Cell adhesion and signalling by cadherins and Ig-CAMs in cancer. *Nat. Rev. Cancer 4*, 118–132.
(47) Ryan, J. A., Overton, K. W., Speight, M. E., Oldenburg, C. M., Loo, L., Robarge, W., Franzen, S., and Feldheim, D. L. (2007) Cellular uptake of gold nanoparticles passivated with BSA-SV40 large T antigen conjugates. *Anal. Chem. 79*, 9150–9159.
(48) Tkachenko, A. G., Xie, H., Liu, Y. L., Coleman, D., Ryan, J., Glomm, W. R., Shipton, M. K., Franzen, S., and Feldheim, D. L. (2004) Cellular trajectories of peptide-modified gold particle complexes: Comparison of nuclear localization signals and peptide transduction domains. *Bioconjugate Chem. 15*, 482–490.

(49) Koudelka, K. J., Rae, C. S., Gonzalez, M. J., and Manchester, M. (2007) Interaction between a 54-kilodalton mammalian cell surface protein and cowpea mosaic virus. *J. Virol. 81*, 1632–1640.

(50) Nagayasu, A., Uchiyama, K., and Kiwada, H. (1999) The size of liposomes: a factor which affects their targeting efficiency to tumors and therapeutic activity of liposomal antitumor drugs. *Adv. Drug Delivery Rev. 40*, 75–87.

(51) Sharma, A., and Sharma, U. S. (1997) Liposomes in drug delivery: progress and limitations. *Int. J. Pharm. 154*, 123–140.

(52) Biffis, A., Orlandi, N., and Corain, B. (2003) Microgel-stabilized metal nanoclusters: Size control by microgel nanomorphology. *Adv. Mater. 15*, 1551–1555.

(53) Morgunova, E. Y., Dauter, Z., Fry, E., Stuart, D. I., Stelmashchuk, V. Y., Mikhailov, A. M., Wilson, K. S., and Vainshtein, B. K. (1994) The atomic structure of carnation mottle virus capsid protein. *FEBS Lett. 338*, 267–271.

(54) Olson, A. J., Bricogne, G., and Harrison, S. C. (1983) Structure of tomato bushy stunt virus. 4. The virus particle at 2.9 Å resolution. *J. Mol. Biol. 171*, 61–93.

(55) Chatterji, A., Ochoa, W. F., Paine, M., Ratna, B. R., Johnson, J. E., and Lin, T. W. (2004) New addresses on an addressable virus nanoblock: Uniquely reactive lys residues on cowpea mosaic virus. *Chem. Biol. 11*, 855–863.

(56) Chatterji, A., Ochoa, W., Shamieh, L., Salakian, S. P., Wong, S. M., Clinton, G., Ghosh, P., Lin, T. W., and Johnson, J. E. (2004) Chemical conjugation of heterologous proteins on the surface of cowpea mosaic virus. *Bioconjugate Chem. 15*, 807–813.

(57) Yoshitake, S., Imagawa, M., Ishikawa, E., Niitsu, Y., Urushizaki, I., Nishiura, M., Kanazawa, R., Kurosaki, H., Tachibana, S., Nakazawa, N., and Ogawa, H. (1982) Mild and efficient conjugation of rabbit Fab' and horseradish peroxidase using a maleimide compound and its use for enzyme immunoassay. *J. Biochem. 92*, 1413–1424.

(58) Steinmetz, N. F., Hong, V., Spoerke, E. D., Lu, P., Breitenkamp, K., Finn, M. G., and Manchester, M. (2009) Buckyballs meet viral nanoparticles: candidates for biomedicine. *J. Am. Chem. Soc. 131*, 17093−+.

(59) Wu, P., and Fokin, V. V. (2007) Catalytic azide-alkyne cycloaddition: Reactivity and applications. *Aldrichim. Acta 40*, 7–17.

(60) Xie, F., Sivakumar, K., Zeng, Q. B., Bruckman, M. A., Hodges, B., and Wang, Q. (2008) A fluorogenic 'click' reaction of azidoanthracene derivatives. *Tetrahedron 64*, 2906–2914.

(61) Zhan, W. H., Barnhill, H. N., Sivakumar, K., Tian, T., and Wang, Q. (2005) Synthesis of hemicyanine dyes for 'click' bioconjugation. *Tetrahedron Lett. 46*, 1691–1695.

(62) Grit, M., and Crommelin, J. A. (1993) Chemical-stability of liposomes - implications for their physical stability. *Chem. Phys. Lipids 64*, 3–18.

(63) Allen, C., Dos Santos, N., Gallagher, R., Chiu, G. N. C., Shu, Y., Li, W. M., Johnstone, S. A., Janoff, A. S., Mayer, L. D., Webb, M. S., and Bally, M. B. (2002) Controlling the physical behavior and biological performance of liposome formulations through use of surface grafted poly(ethylene glycol). *Biosci. Rep. 22*, 225–250.

(64) Charrois, G. J. R., and Allen, T. M. (2004) Drug release rate influences the pharmacokinetics, biodistribution, therapeutic activity, and toxicity of pegylated liposomal doxorubicin formulations in murine breast cancer. *Biochim. Biophys. Acta 1663*, 167–177.

(65) Lee, R. J., Wang, S., Turk, M. J., and Low, P. S. (1998) The effects of pH and intraliposomal buffer strength on the rate of liposome content release and intracellular drug delivery. *Biosci. Rep. 18*, 69–78.

(66) Schroeder, A., Avnir, Y., Weisman, S., Najajreh, Y., Gabizon, A., Talmon, Y., Kost, J., and Barenholz, Y. (2007) Controlling liposomal drug release with low frequency ultrasound: Mechanism and feasibility. *Langmuir 23*, 4019–4025.

(67) Lee, H. I., Wu, W., Oh, J. K., Mueller, L., Sherwood, G., Peteanu, L., Kowalewski, T., and Matyjaszewski, K. (2007) Light-induced reversible formation of polymeric micelles. *Angew. Chem., Int. Ed. 46*, 2453–2457.

(68) Tkachenko, A. G., Xie, H., Coleman, D., Glomm, W., Ryan, J., Anderson, M. F., Franzen, S., and Feldheim, D. L. (2003) Multifunctional gold nanoparticle-peptide complexes for nuclear targeting. *J. Am. Chem. Soc. 125*, 4700–4701.

(69) Liu, Y. L., and Franzen, S. (2008) Factors determining the efficacy of nuclear delivery of antisense oligonucleotides by gold nanoparticles. *Bioconjugate Chem. 19*, 1009–1016.

BC100361Z